Factors influencing $CaCO_3$ scale precipitation and CO_2–H_2O system in flowing water in natural water piping system

Aiman E. Al-Rawajfeh

Tafila Technical University, Department of Chemical Engineering, P.O. Box 179, 66110 Tafila, Jordan
*Tel. +962 (3) 2250034; Fax +962 (3) 2250431; email: aimanr@yahoo.com*

ABSTRACT

This work considers the factors influencing $CaCO_3$ scale precipitation and CO_2–H_2O system for flowing water in steel pipes. An experimental setup is used to simulate the pumping system of water supply in natural water piping system in which a certain amount of water is pumped at a certain pH, temperature, and flow rate as initial conditions. The pH values, temperatures and flow rates increase with the time of circulation of 5 h of each run. The pH of the water samples ranged from 7.2 to 8.0 and temperatures increase by 18–20°C when the flow rates change from 43.3 to 58.3 L/min, respectively. Water samples investigated in this study exhibit high concentration of Cl^-, SO_4^{2-} and HCO_3^- as the major anions and Ca^{2+} as the major cation. Saturation ratio of calcite ($\Omega_{calcite}$) increases from 0.03 to 0.10 units, consequently, the amount of scale precipitation increases from 0.2 to 0.4 mg $CaCO_3$/kg of feed water. The concentrations of HCO_3^- and CO_3^{2-} decrease from initial to final conditions, while the concentration of CO_2 increases. The saturation with respect to CO_2 was found to be very low and decreases with increasing flow rate and temperature, this implies that CO_2 is released from the water, leading to an increase in the pH value and thereby increasing the possibility for $CaCO_3$ to precipitate.

Keywords: $CaCO_3$ precipitation; Natural water; Piping system; Flow rate

1. Introduction

The crystallization of the calcium carbonate ($CaCO_3$) or scale formation strongly depends on temperature, pH, desorption rate of CO_2 as well as on the concentrations of HCO_3^-, CO_3^{2-}, Ca^{2+}, and water chemistry as a whole [1]. The temperature sensitivity of the various constants of the $CaCO_3$–CO_2–H_2O system results in the following net reaction being driven to the right with increasing temperature:

$$Ca^{2+} + 2\,HCO_3^- \xleftarrow{\quad k_r \quad} CaCO_3\,(s) + CO_2 + H_2O \qquad (1)$$
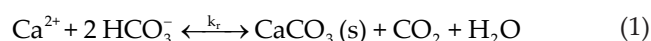
The thermodynamic driving force for calcium carbonate crystallization either in the bulk or at the pipe wall is defined as the difference of Gibbs free energy between the supersaturated state and equilibrium:

$$\Delta G = -RT \ln \Omega \qquad (2)$$

where R is the gas constant, T is the absolute temperature and Ω is the supersaturation ratio of the crystalline precipitate.

$CaCO_3$ precipitates into three polymorphic forms: aragonite, calcite and vaterite. Aragonite (needle-shaped), calcite (cubic) and vaterite (spherically-shaped) have different solubility properties, vaterite being the most and calcite the least soluble phase over a temperature range between 0°C and 90°C [2]. $CaCO_3$ precipitates spontaneously when the temperature rises, reducing solubility of $CaCO_3$ and upon the desorption of CO_2 resulting in pH increase and therefore causes concentration gradient [1]. The crystallization of the $CaCO_3$ involves three basic

stages [3]: (i) ions start to cluster as proto-nuclei of up to 1000 atoms as the ion concentration increases; (ii) the proto-nuclei grow as concentration increases and the ions start ordering themselves into a regular shape and (iii) finally, crystals are formed from the nuclei. Once formed, the crystals continue to grow indefinitely as long as the respective salt solubility limit is exceeded.

$CaCO_3$ deposition rates in the flow of cooling towers and heat exchangers, in which scale-producing water falling film is evaporated on the outside surface of a vertical cylindrical tube, have been modeled by Hasson and Perl [4] and Chan and Ghassemi [5,6]. Tanaka et al. [7] has modeled $CaCO_3$ deposition rates in flow into irrigation systems. However, these models are not of general-purpose because: they are one-dimensional fluid analysis, the chemistry of the solution was not taken into account comprehensively in the description of the models, the CO_2 desorption was not treated enough and limiting the study on $CaCO_3$ precipitation on the wall surface. The precipitation on the phase interface and in the liquid bulk has not been taken into account.

The $CaCO_3$ scaling and corrosion in industrial processes is affected by the following factors [8,9]: (i) bulk variables and composition, i.e. $CaCO_3$ precipitation potential, pH buffering capacity, chloride and sulfate concentrations and concentration of dissolved oxygen, (ii) thermal effect, i.e. heat flux, surface temperature and bulk temperature, (iii) flow field, i.e. velocity of flow and solid/liquid interface conditions and (iv) substrate properties, i.e. materials properties and surface conditions.

This work aims at studying the factors influencing $CaCO_3$ scale precipitation and CO_2–H_2O system in flowing water in natural water piping systems. The pumping of water from the main source to the houses through a steel-pipes network is simulated in a laboratory experiment.

2. Experimental

The experimental work has been conducted using a computer controlled EDIBON (Spain) series/parallel pumps system as shown in Fig. 1. This setup is used to simulate the pumping system of water network supply to the houses around Tafila Technical University from the National Water Authority in Tafila Province, south Jordan which is supplied from Zabda Well. A certain amount of water (~20 L for each run) is transferred to the water tank from the tap which comes from the University main tank after getting rid from the first few liters in the network. Galvanized steel (22 mm diameter) with flow path length of around 4 m in total including 20 cm glass section is used. The temperature, flow rate, pH and EC are recorded and then a sample is taken to the analysis. Then the pumps are switched on to begin the experiment at a certain initial conditions of pH, temperature and flow rate. The duration of each experiment was 5 h. The tem-
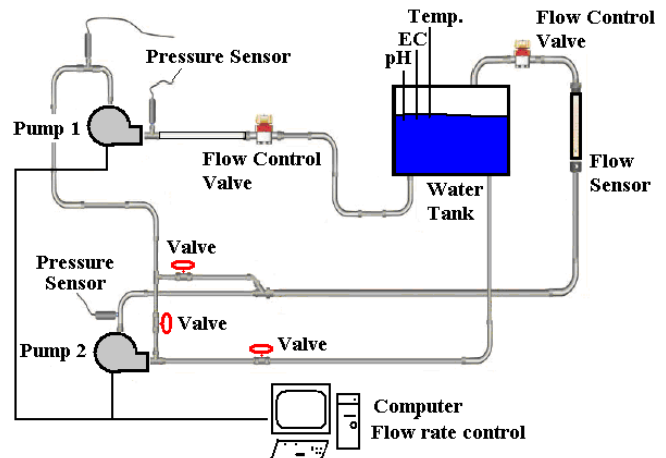

Fig. 1. Experimental setup (a computer controlled EDIBON series/parallel pump system).

perature, flow rate, pH and EC at the end are recorded and a sample is taken to the analysis.

The water samples were collected in polyethylene bottles. pH and electrical conductivity (EC) were measured using CG 712 (SCHOTT GERAETE) pH meter and ORION model 162 conductivity meter, respectively. The samples were also analyzed for major cations and anions; K^+, Na^+ and Ca^{2+} were analyzed using an ATS 200 MKI (Advanced Technical Service) flame photometer. F^-, Cl^-, NO_3^- and SO_4^{2-} were analyzed using ion chromatography (Dionex-100 with an AG4A-SC guard column, AS4SC separating column, an SSR1 anion self-regenerating suppressor and a conductivity meter).

3. Results and discussion

The temperature, pH, electrical conductance (EC), total dissolved solids (TDS), total alkalinity (TA), total carbon dioxide (TC), the major ionic composition, the saturation ratio of $CaCO_3$ as calcite, the excess carbon dioxide pressure ($EpCO_2$) and the calcium carbonate precipitation potential (CCPP) of the initial and final water samples at initial and final conditions are summarized in Table 1. If TA and pH of water samples are given, the concentrations of HCO_3^-, CO_3^{2-}, and CO_2 species can be determined by calculating $[H^+]$ from the pH value. Then, other species can be calculated as follows:

$$[OH^-] = K_W / [H^+] \tag{3}$$

$$[HCO_3^-] = \frac{TA + [H^+] - [OH^-]}{(1 + 2K_2 / [H^+])} \tag{4}$$

$$[CO_2^*] = \frac{TA + [H^+] - [OH^-]}{K_1 / [H^+](1 + 2K_2 / [H^+])} \tag{5}$$

Table 1
Temperature, pH, electrical conductance (EC), total dissolved solids (TDS), the major ionic composition, the saturation ratio of $CaCO_3$ as calcite, the excess carbon dioxide pressure ($EpCO_2$) and the calcium carbonate precipitation potential (CCPP) for the water samples

Species	Condition					
	Initial	Final	Initial	Final	Initial	Final
Flow rate, L/min	43.3	44.8	49.6	51.8	53.8	58.3
Temperature, °C	13.0	32.0	17.0	35.0	18.0	38.0
pH	7.5	7.7	7.4	7.8	7.6	8.0
EC, mS/cm	114.5	115.4	112.3	113.9	113.0	112.7
TDS, ppm	73.28	73.86	71.87	72.90	72.32	72.13
TA, mmol/kg	128.3	128.3	133.9	128.3	133.9	128.3
TC, mmol/kg	130.5	127.5	137.8	126.0	134.6	122.8
Na^+, ppm	15	14.7	14.7	14.7	14.3	15.3
K^+, ppm	2.2	2.2	2	2.1	2.2	2.1
Ca^{2+}, ppm	23	23	24	23	24	23
F^-, ppm	0.3	0.3	0.3	0.3	0.4	0.3
Cl^-, ppm	71.8	63.6	60.9	64	57.6	62
NO_3^-, ppm	24.6	21.8	19.9	20.6	19	20.3
SO_4^{2-}, ppm	25	22.1	21.2	22.4	20.5	22
HCO_3^-, mmol/kg	124.6	122.4	130.8	120.9	129.0	116.9
CO_3^{2-}, mmol/kg	1.54	2.41	1.29	2.99	2.02	4.58
CO_2, mmol/kg	4.38	2.70	5.77	2.12	3.59	1.30
$\Omega_{calcite}$	0.169	0.212	0.155	0.235	0.194	0.291
$EpCO_2$, ppm×107	6.56	4.07	8.68	3.19	5.40	1.95
CCPP, mg/kg	−4.88	−4.66	−4.95	−4.56	−4.70	−4.32
(SO_4/HCO_3), mM	2.1	1.9	1.7	1.9	1.7	2.0
$(Cl+SO_4)$, ppm	96.8	85.7	82.1	86.4	78.1	84

$$[CO_3^{2-}] = \frac{TA + [H^+] - [OH^-]}{2(1 + [H^+]/2K_2)} \qquad (6)$$

$$TC = [HCO_3^-] + [CO_3^{2-}] + [CO_2^*] \qquad (7)$$

$$TA = [HCO_3^-] + 2[CO_3^{2-}] + [OH^-] - [H^+] \approx [HCO_3^-] \qquad (8)$$

where K_1, K_2 and K_W are the first and second dissociation and ionization constants of carbonic acid and water, respectively.

The experiments were conducted at different initial flow rates and the final conditions were recorded. The initial flow rates were 40.2, 43.3, 49.6, and 53.8 L/min. After circulating the water in the system for 5 h, the final conditions were recorded. The final-condition flow rates increased to 43.4, 44.8, 51.8, and 58.3 L/min, for the corresponding initial values, respectively. This may be attributed to the increase in temperature because of friction and consequently the decrease of water viscosity.

The pH of the water samples ranged from 7.2 at initial conditions to 8.0 at final conditions. Water samples temperatures increase from 12.0 to 30.0°C when the flow rate changes from 40.2 to 43.4 L/min, the change in temperature ranged from 18–20°C and the maximum temperature reached at 58.3 L/min is 38.0°C. Water samples investigated in this study exhibit high concentration of Cl^-, SO_4^{2-} and HCO_3^- as the major anions and Ca^{2+} as the major cation. Corrosive behavior of metals in aqueous solutions is mainly determined by dissolved salts and oxygen. Chloride ions (for all samples in this work, (Cl + SO_4) > 50 ppm) increase the electrical conductivity of water, facilitate the flow of corrosion current, and simultaneously, hinders the creation of protection layers. They also contribute to nucleation and propagation of corrosion pits. Additionally, Cl^- ions create dissolving salts with most of metals and therefore protection layers made of corrosion products are not created. CO_2 (due to its acidic character) in water may influence corrosion directly and indirectly by creating protection layers of calcium carbonate. It is known that the solubility of carbonate and bicarbonate ions increases in the presence of excess chloride ions. Thus, the molar ratio of SO_4/HCO_3 is a predictive ratio to the type of the scale, if it is either SO_4 or CO_3 scale [10]. A value less than 1 indicates high CO_3 scale (i.e. >80%) and low SO_4 scale while a value between

1 to 10 indicates medium to high CO_3 scale and medium SO_4 scale. The SO_4/HCO_3 ratios of the water samples were found to be greater than 1.

The supersaturation ratio of the crystalline precipitate (calcite) is defined as

$$\Omega_{calcite} = \left(\frac{[Ca^{2+}][CO_3^{2-}]}{K_{sp,cal}} \right)^{\frac{1}{2}} \tag{9}$$

where K_{sp} is the thermodynamic solubility product of the dominant polymorph (calcite). Supersaturation, in this work, is computed with respect to calcite because it is found to be the predominant crystalline deposit for temperatures below 35°C [10] and lower supersaturation [12].

Fig. 2 shows the relationship between pH, TC and the equilibrium concentration of Ca^{2+} with respect to $CaCO_3$. The equilibrium concentration of Ca^{2+} can be calculated by solving the following equation [13]:

$$[Ca^{2+}]^2 - \left\{ \frac{[H^+]^2 + K_W}{2[H^+]} + \frac{TC}{2} \left(\frac{K_1 K_2}{K_1[H^+] + K_1 K_2 + K_2[H^+]} \right) \right\}$$
$$\cdot [Ca^{2+}] - K_{sp,cal} = 0 \tag{10}$$

For example, if Ca^{2+} concentration is 10^{-4} and TC is 10^{-2}, the solution becomes saturated with respect to $CaCO_3$ at pH = 8.2, i.e. if the pH value increases to a value above 8.2, the water will be considered supersaturated such that $CaCO_3$ may begin to precipitate. Consideration of only Ca^{2+} in the $CaCO_3$ precipitation is inaccurate [14] because calcium ions may be paired with SO_4^{2-}, HCO_3^-, CO_3^{2-}, PO_4^{3-} and other species. This leads to overestimating the forming amount of $CaCO_3$. The participation of CO_2, HCO_3^-, CO_3^{2-} (which are affected by the pH of the solu-

tion) should be accounted for by correlating the $CaCO_3$ deposition rates to the CO_2 release and the change in total alkalinity, i.e. CCPP. The pH increased due to the release of CO_2 and scale precipitation.

The calcium carbonate precipitation potential (CCPP) [15] is a parameter that predicts the tendency to precipitate or to dissolve $CaCO_3$ in addition to its quantity as well. CCPP can be calculated from the initial total alkalinity (TA_i) and equilibrium total alkalinity (TA_{eq}) with computerised water chemistry models according to the following relationship [14–17]:

$$CCPP = EqWt_{CaCO_3} (TA_i - TA_{eq}) \tag{11}$$

where EqWt is the equivalent weight of $CaCO_3$ (EqWt = 50,000 mg/mol), TA_i and TA_{eq} are the initial and equilibrium (or final) total alkalinity, respectively. CCPP is proportional to the reaction kinetics according to the following relationship [17]. The decrease in calcium ions concentration is proportional to the amount of $CaCO_3$ precipitation:

$$\frac{d[Ca^{2+}]}{dt} = -10^{-5} k_r A (CCPP)^2 \tag{12}$$

where k_r is the rate constant of reaction (1), $k_r = 9.496 \times 10^{19}$ exp $(-4800/T)$ [5,6], and A is the surface area available for precipitation.

Fig. 3 shows the amount of $CaCO_3$ may dissolve or precipitate (CCPP) in mg per kg of the feed water with increasing the temperature. The deposition amount of $CaCO_3$ increases with increasing the flow rate; this is attributed to the change in temperature. The differences in the temperature increase from 18, 19 to 20°C units when the flow rates change from 43.3 to 44.8, 49.6 to 51.8 and 53.8 to 58.3 L/min, respectively.
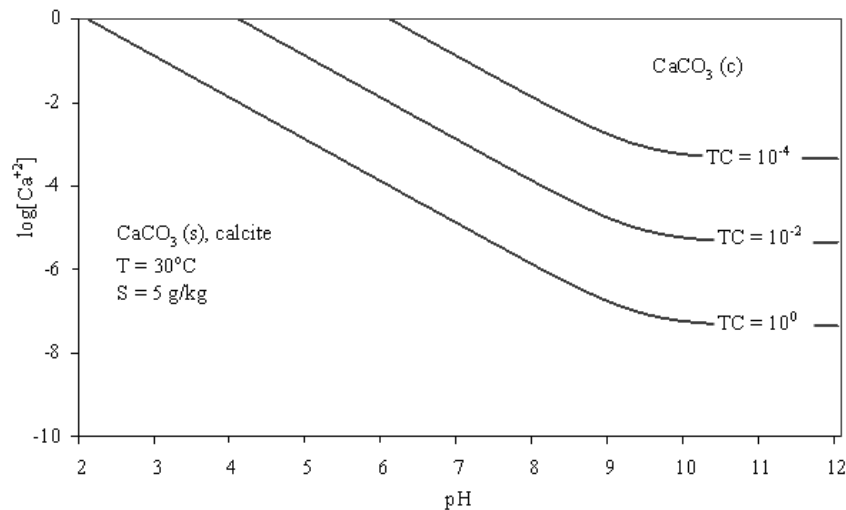

Fig. 2. Logarithmic concentration diagram showing the relationship between pH, TC and the equilibrium concentration of Ca^{2+} with respect to $CaCO_3$.
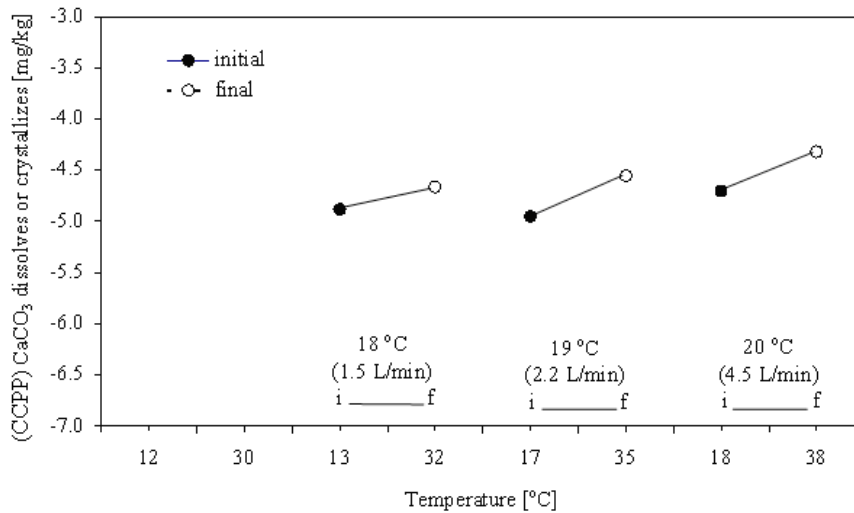
Fig. 3. Amount of $CaCO_3$ may dissolve or crystallize (CCPP) in mg/kg of the feed water vs. temperature.

Fig. 4 shows the influence of flow rate on $CaCO_3$ deposition. It is evaluated by chemical analysis of the water sample at the initial and final conditions. The amount of $CaCO_3$ deposition increases with increasing the flow rate, i.e. higher flow rate brings more ions for the precipitation process. Moreover, turbulent flow can produce the necessary activation energy for the precipitation process [18]. This result is supported by the values of saturation ratio. Saturation ratio of calcite ($\Omega_{calcite}$) increases with increasing the flow rate from 0.03, 0.08 and 0.10 units for initial flow rates of 43.3, 49.6 and 53.8 L/min, respectively.

When a certain total carbon dioxide content (TC) is dissolved in water, it is important to know which fraction thereof is present as CO_2, which as HCO_3^- ions and which as CO_3^{2-} ions. The distribution of the species depends on the pH value, the temperature and the ionic strength. The ratios of individual CO_2–H_2O species can be given as:

$$\alpha_{CO_2} = \frac{[CO_2]}{TC} = \frac{1}{1 + K_1/[H^+] + K_1 K_2/[H^+]^2} \tag{13}$$

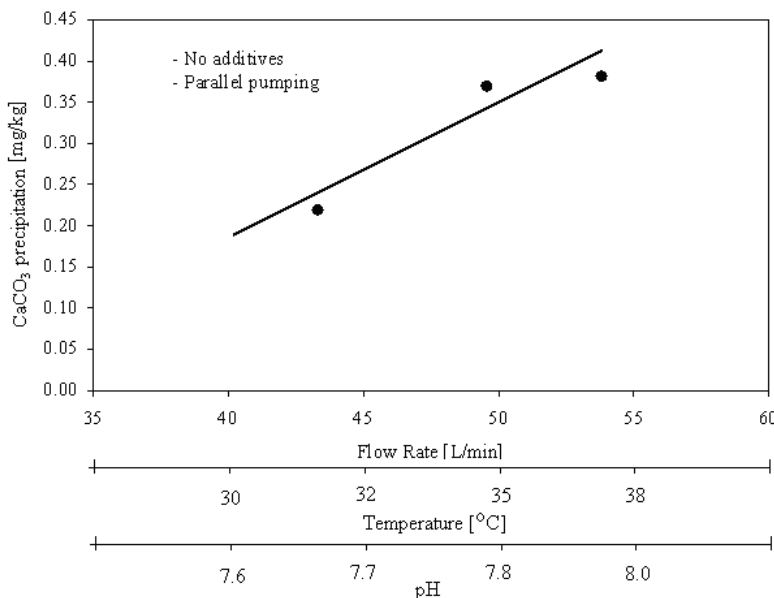$$\alpha_{HCO_3} = \frac{[HCO_3^-]}{TC} = \frac{1}{1 + [H^+]/K_1 + K_2/[H^+]} \tag{14}$$

Fig. 4. Factors influencing $CaCO_3$ precipitation. They are evaluated by chemical analysis of the water sample at the initial and final conditions.

$$\alpha_{CO_3^{2-}} = \frac{[CO_3^{2-}]}{TC} = \frac{1}{1+[H^+]/K_2 +[H^+]^2/K_1K_2} \qquad (15)$$

Fig. 5A shows a log C-pH diagram ($C = CO_2$, HCO_3^-, CO_3^{2-} and saturation value of $[Ca^{2+}]$) of the $CaCO_3$–CO_2–H_2O system as a function of pH. HCO_3^- intersects with CO_2 and CO_3^{2-} at the system points. The concentrations of HCO_3^- and CO_3^{2-} decrease from initial to final conditions while the concentration of CO_2 increases as shown in Fig. 5B, Fig. 5D and Fig. 5C, respectively. The concentration of HCO_3^- decreases because of the thermal decomposition producing CO_2 and CO_3^{2-} according to Eq. (1). Under these conditions, CO_2 is released from the water leading to an increase in the pH value (Table 1) and thereby increasing the possibility for $CaCO_3$ to precipitate, i.e. the concentration of CO_3^{2-} decreases because it combines with Ca^{2+} to produce $CaCO_3$. To prove that most of the amount CO_2 is released, the saturation with respect to CO_2 can be calculated from Neal et al. [19]:

$$EpCO_2 = \left([10^3 \, Alk/61] \cdot 10^{(6-pH)}\right)/6 \qquad (16)$$

where $EpCO_2$ is excess carbon dioxide pressure and Alk is the alkalinity, in ppm bicarbonate.

Based on this equation, $EpCO_2$ values were found to be very small (i.e. in the range of 10^{-7} ppm) as shown in Table 1.

4. Conclusion

The influencing factors on $CaCO_3$ precipitation and CO_2–H_2O system in flowing water in natural water steel piping systems were investigated. The initial factors were increased by circulating the water samples for 5 h in a system simulating the piping system. The factors are pH, temperature and flow rate. The pH values, temperatures and saturation ratio of calcite ($\Omega_{calcite}$) of the water samples increased from the initial to the final flow rates conditions. Water samples temperatures increased by 18–20°C.
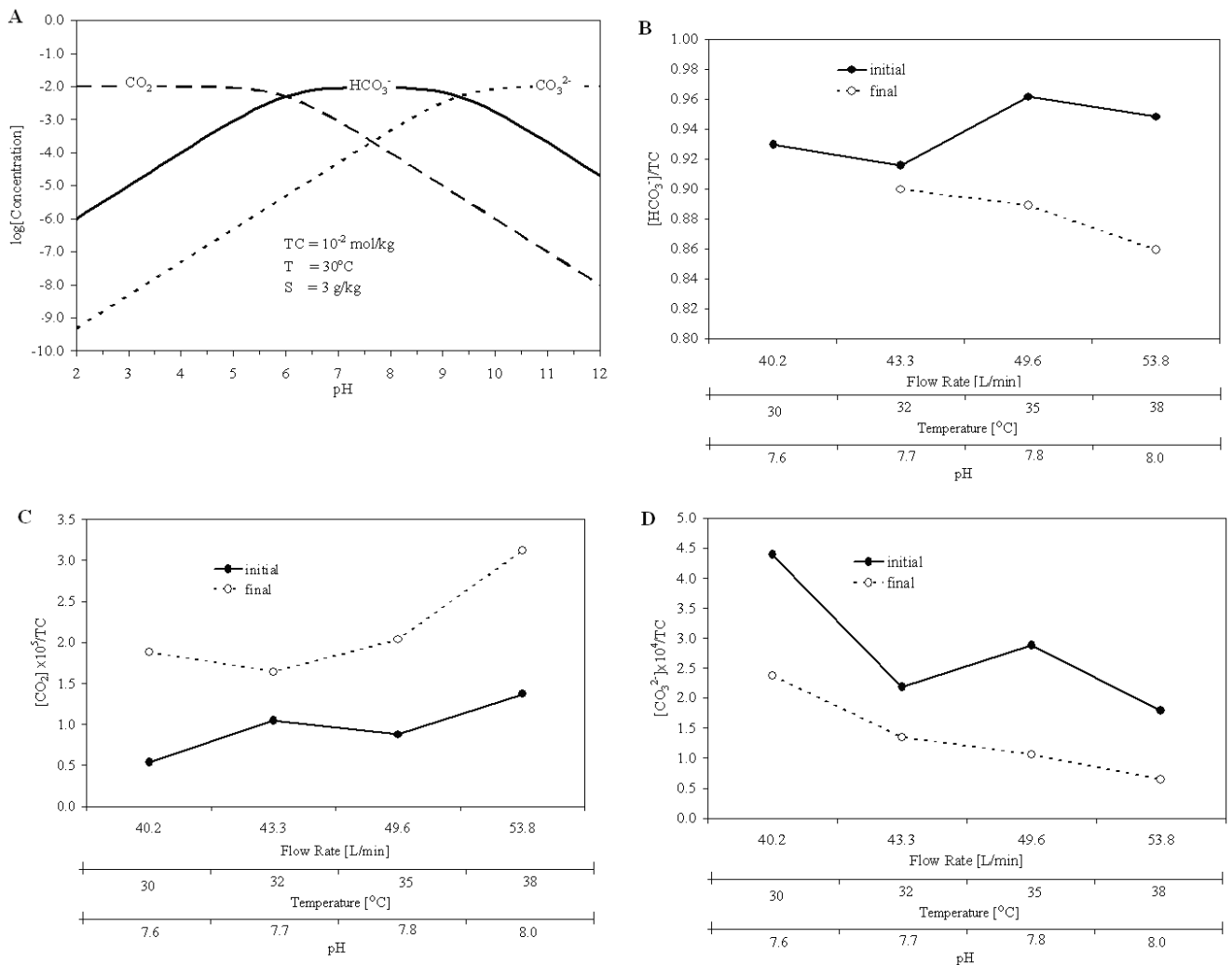

Fig. 5. Changes in CO_2–H_2O species ratios with the initial flow rate and final pH and temperature, A: log C–pH diagram ($C = CO_2$, HCO_3^- and CO_3^{2-}), B: Change in $[HCO_3^-]$, C: Change in $[CO_2]$, D: Change in $[CO_3^{2-}]$.

The concentrations of HCO_3^- and CO_3^{2-} decreased from the initial to final conditions while the concentration of CO_2 increased. The saturation with respect to CO_2 was found to be in a magnitude that implies that most of CO_2 is released from the water, leading to an increase in the pH value. However, the amount of $CaCO_3$ precipitation increased with increasing the initial pH, temperature and flow rate. The pH increased due to the release of CO_2 and scale precipitation.

Acknowledgement

Symbols

A	—	Area, m^2
Alk	—	Alkalinity, ppm bicarbonate
CO_3^{2-}	—	Carbonate ion
$EpCO_2$	—	Excess carbon dioxide pressure, ppm
HCO_3^-	—	Bicarbonate ion
H_2CO_3	—	Carbonic acid
$[i]$	—	Concentration of the component i, mol/kg solution
K_1	—	First dissociation constant of carbonic acid in water on the basis mol/kg solution
K_2	—	Second dissociation constant of carbonic acid in water on the basis mol/kg solution
K_{sp}	—	Solubility product constant of calcium carbonate in water on the basis mol^2/kg^2 solution
k_r	—	Rate constant of the forward reaction. For first order, the unit is 1/s
OH^-	—	Hydroxide ion
pH	—	pH value
R	—	Gas constant, J/mol.K
T	—	Temperature, K
TA	—	Total alkalinity, mol/kg
TC	—	Total carbon dioxide content, mol/kg

Greek

α	—	Species ratio
Ω	—	Supersaturation ratio

Indices

eq	—	Chemical equilibrium
i	—	Component
r	—	Reaction

References

[1] A.E. Al-Rawajfeh, H. Glade and J. Ulrich, Scaling in multiple-effect distillers: the role of CO_2 release. Desalination, 182 (2005) 209–219.
[2] M.E.Q. Pilson, An Introduction to the Chemistry of the Sea. Prentice-Hall Inc., New Jersey, 1998.
[3] E.G. Darton, Scale inhibition techniques used in membrane systems. Desalination, 113 (1997) 227–229.
[4] D. Hasson and I. Perl, Scale deposition in a laminar falling-film system, Desalination, 37 (1981) 279–292.
[5] S.H. Chan and K.F. Ghassemi, Analytical modeling of calcium carbonate deposition for laminar falling film and turbulent flow in annuli: Part I – Formulation and single-species model, ASME J. Heat Transfer, 113 (1991) 735–740.
[6] S.H. Chan and K.F. Ghassemi, Analytical modeling of calcium carbonate deposition for laminar falling film and turbulent flow in annuli: Part II – Multispecies model, ASME J. Heat Transfer, 113 (1991) 741–746.
[7] Y. Tanaka, A. Mukai and T. Naka, Prediction of $CaCO_3$ scale in the flow into irrigation system — the simulation of the effect of the pressure based on Lagrange fluid analysis. 1st IWA Conference on Scaling and Corrosion in Water and Wastewater Systems, Cranfield University, UK, 25–27 March 2003.
[8] A.J. Karabelas, Scale formation — Some key unresolved issues. In: Scaling in Seawater Desalination: Is molecular Modeling the Tool to Overcome the Problem? G. Glade and J. Ulrich, eds., Aachen, Shaker Velag, 2001, pp. 117–137.
[9] R.E. Loewenthal, I. Morrison and M.C. Wentzel, Control of corrosion and aggression in drinking water systems. 1st IWA Conference on Scaling and Corrosion in Water and Wastewater Systems, Cranfield University, UK, 25–27 March 2003.
[10] S. El-Manharawy and A. Hafez, Molar ratios as a useful tool for prediction of scaling potential inside RO systems, Desalination, 136 (2001) 243–254.
[11] N. Andritsos and A.J. Karabelas, Calcium carbonate scaling in a plate heat exchanger in the presence of particles, Int. J. Heat Mass Trans., 46 (2003) 4613–4627.
[12] C.W. Turner and D.W.M. Smith, Calcium carbonate scaling kinetics determined from radiotracer experiments with calcium-47, Ind. Eng. Chem. Res., 37 (1998) 439–448.
[13] C.N. Sawyer, P.L. McCarty and G.F. Parkin, Chemistry for Environmental Engineering, McGraw Hill, New York, 1994.
[14] A.E. Al-Rawajfeh, Modeling of alkaline scale formation in falling film horizontal-tube multiple-effect distillers, Desalination, 205 (2007) 124–139.
[15] J.R. Rossum and D.T. Merrill, An evaluation of the calcium carbonate saturation indexes, J. AWWA, 75 (1983) 95–100.
[16] R.E. Loewenthal, G.A. Ekama and G.vR. Marais, STASOFT: A user-friendly interactive computer program for softening and stabilisation of municipal waters, Water SA, 14 (1988) 159–162.
[17] V.L. Snoeyink and [initials??] Jenkins, Water Chemistry, John Wiley and Sons, New York, 1980.
[18] B. Kaasa and T. Ostvold, Prediction of pH and mineral scaling in water with varying ionic strength containing CO_2 and H_2S for $0 < T$ (°C) < 200 and $1 < P$ (bar) 500, Proc. Advances in Solving Oilfield Scaling, Abredeen, UK, January 28–29, 1998.
[19] C. Neal, W. Alanouse and K. Down, An assessment of excess carbon dioxide partial pressures in natural waters based on pH and alkalinity measurements, Sci. Total Environ., 210–211 (1998) 173–185.